



**HAL**  
open science

## Developments to improve the stability of optical lattice clocks

S. Bize, B. Fang, Y. Le Coq, R. Le Targat, J. Lodewyck, P.-E. Pottie, H. Shang, C. Zyskind

► **To cite this version:**

S. Bize, B. Fang, Y. Le Coq, R. Le Targat, J. Lodewyck, et al.. Developments to improve the stability of optical lattice clocks. *Journal of Physics: Conference Series*, 2024, 2889 (1), pp.012048. 10.1088/1742-6596/2889/1/012048 . hal-04796895

**HAL Id: hal-04796895**

**<https://hal.science/hal-04796895v1>**

Submitted on 22 Nov 2024

**HAL** is a multi-disciplinary open access archive for the deposit and dissemination of scientific research documents, whether they are published or not. The documents may come from teaching and research institutions in France or abroad, or from public or private research centers.

L'archive ouverte pluridisciplinaire **HAL**, est destinée au dépôt et à la diffusion de documents scientifiques de niveau recherche, publiés ou non, émanant des établissements d'enseignement et de recherche français ou étrangers, des laboratoires publics ou privés.



Distributed under a Creative Commons Attribution 4.0 International License

PAPER • OPEN ACCESS

## Developments to improve the stability of optical lattice clocks

To cite this article: S. Bize *et al* 2024 *J. Phys.: Conf. Ser.* **2889** 012048

View the [article online](#) for updates and enhancements.

You may also like

- [Atom Fountains at NTSC](#)  
Jun Ruan, Xinliang Wang, Hui Zhang et al.
- [High-accuracy multi-ion spectroscopy with mixed-species Coulomb crystals](#)  
J. Keller, H. N. Hausser, I. M. Richter et al.
- [REFIMEVE frequency and time network and applications](#)  
E Cantin, O Lopez, C Chardonnet et al.



The Electrochemical Society  
Advancing solid state & electrochemical science & technology

**247th ECS Meeting**  
Montréal, Canada  
May 18-22, 2025  
*Palais des Congrès de Montréal*

**Abstracts due December 6th**

**Showcase your science!**

**ECS UNITED**

# Developments to improve the stability of optical lattice clocks

**S. Bize, B. Fang, Y. Le Coq, R. Le Targat, J. Lodewyck, P.-E. Pottie, H. Shang, and C. Zyskind**

LNE-SYRTE, Observatoire de Paris - PSL, CNRS, Sorbonne Université,  
61 avenue de l'Observatoire, 75014 Paris, France.

E-mail: [sebastien.bize@obspm.fr](mailto:sebastien.bize@obspm.fr)

## Abstract.

We present several developments aimed at improving the stability of optical lattice clocks. First, we present our developments of an optical lattice clock using neutral mercury. We mention recent advances made with the fermionic isotope  $^{199}\text{Hg}$ . We also mention our work aimed at using bosonic isotopes, which offer the possibility to circumvent the relatively short lifetime of the upper clock state in  $^{199}\text{Hg}$ . Second, we present our work on a non-destructive detection in a Sr optical lattice clock. We describe developments that brought the detection scheme from the classical non-destructive regime to the quantum non-destructive regime. Our detection scheme is practical and has the capability to be used beyond proving the principle. Finally, we present our work on laser stabilization using spectral hole burning in a  $\text{Eu}^{3+}:\text{Y}_2\text{SiO}_5$  crystal at cryogenic temperatures. We describe our development of low noise interrogation based on digital IQ modulation and detection that can probe multiple spectral features simultaneously, as well as several investigations towards fluctuating environmental factors. These advances, individually or combined for example with spectral purity transfer with combs and composite clock approaches, shall bring significant progress in clock stability and accuracy.

## 1. Progress in the development of a Hg lattice clock

Neutral mercury Hg offers the possibility to develop an optical lattice clock with a low sensitivity to thermal radiation and to stray electric fields. Hg is about  $\sim 30$  times less sensitive than Sr and  $\sim 15$  times less sensitive than Yb. Highly accurate measurements of frequency ratios between Hg and other optical transitions can bring interesting contributions to fundamental physics tests and metrology. Our group, and the group at University of Tokyo and RIKEN, studied optical lattice clock based in the fermionic isotope  $^{199}\text{Hg}$ . These developments gave two accurate and independent measurements of the frequency ratio  $^{199}\text{Hg}/^{87}\text{Sr}$  with uncertainties of  $1.8 \times 10^{-16}$  [1] and  $8.4 \times 10^{-17}$  [2] in agreement with the  $1\sigma$  error bar. Both measurements were limited by the systematic uncertainties of the  $^{199}\text{Hg}$  systems. Our group also made direct measurement of the absolute frequency, i.e. of the  $^{199}\text{Hg}/^{133}\text{Cs}(\text{hfs})$  ratio, and of the  $^{199}\text{Hg}/^{87}\text{Rb}(\text{hfs})$ . In 2017, these measurements led CIPM to recommend the  $^1\text{S}_0\text{-}^3\text{P}_0$  in  $^{199}\text{Hg}$  as a secondary representation of the SI second [3]. In the 2021 update of the list of recommended frequencies and secondary representations of the second [4][5], still based on the two aforementioned measurements, the  $^{199}\text{Hg}$  clock transition has a recommended fractional uncertainty of  $2.4 \times 10^{-16}$ , not far from the best recommended uncertainty ( $1.9 \times 10^{-16}$  for  $^{87}\text{Sr}$ ,  $^{171}\text{Yb}$ ,  $^{171}\text{Yb}^+(\text{E}3)$  and  $^{27}\text{Al}^+$ ) which



is determined by the uncertainty of the realisation of the SI second by cesium fountains.

Main limitations of our work with  $^{199}\text{Hg}$  were the following. A first limit was the uncertainty to which we were able to control the optical frequency of our optical lattice light with a commercial lambdameter. A second limit was a relatively modest lattice trap depth (estimated to  $\sim 56$  recoil energy  $E_R$ ) owing to the challenging UV wavelength (362.5 nm [6]) and the comparatively low polarizability (a price to pay for the low blackbody radiation sensitivity). Another limit was the short term stability that we could achieve ( $> 1.2 \times 10^{-15}$  at 1s). This limit was itself linked to several factors: a limited number of atoms that could be captured in a given time and a rather short lifetime of the atomic sample in the lattice trap, which together impose a duty cycle of the probing sequence no better than  $\sim 10\%$  and increase the impact of the Dick effect. The reliability of our Hg clock system was also significantly limiting our capability to perform and repeat long measurement sessions, the main factor being the 254 nm light source for cooling and detecting atoms. Another limit was coming from residual background gases in our vacuum system which contribute to limit the lifetime of the atomic sample trapped in the lattice and cause a background collision shift. The impact of the latter was found quite significant in recent studies on  $^{171}\text{Yb}$  and  $^{87}\text{Sr}$  [7][8].

Next, we mention several developments to improve over these limits. First, we developed a system to drastically improve the control of the lattice trap frequency. Our approach was to lock the lattice light frequency to a comb in order to have virtually no limit to the level of control. We aimed to do this with the same metrological comb already used to link the Hg clock light at 1062.5 nm (282.1 THz, one fourth of the  $^1\text{S}_0$ - $^3\text{P}_0$  transition frequency). To do this, we relied on a 1450 nm extended cavity diode laser (ECDL) which the frequency doubled to obtain a beat note against the 725 nm light (TiSa laser) frequency doubled to generate the optical lattice trap light at 362.5 nm. 1450 nm is a wavelength where our fiber based comb have, without any modification, enough power to obtain a beat note signal. To use these beat notes and lock frequency of the 1450 nm laser comb and the TiSa laser to the doubled 1450 nm laser, we developed a locking scheme tolerant to extremely low signal-to-noise ratios while remaining sufficiently accurate, avoiding any further requirement to the comb in terms of power in the relevant spectral region. We estimated that our system can control the absolute frequency of our lattice light to an uncertainty of  $\sim 1$  kHz, which should not be a limit to the accuracy of our Hg clock down to  $10^{-18}$  or even better [9]. Second, we improved our laser sources for cooling and detecting the atoms with the  $^1\text{S}_0$ - $^3\text{P}_1$  transition at 254 nm to allow for practical 2 dimensional magneto-optical trap (2D-MOT), a possibility arising from the high vapour pressure of mercury, which had not been exploited before. Our system comprises two independent generation of 254 nm light, each with a home-built ECDL at 1015 nm seeding a commercial Yb fiber amplifier and single pass doubling to 508 nm followed by a home-built cavity-enhanced frequency doubling to 254 nm [10]. One of the light source is stabilized to Doppler-free absorption spectrum from a room temperature 1 mm long Hg vapor cell. The second light source is frequency stabilized to the first one via an optical beat note at 1015 nm, providing independent frequency tuning of the two sources. One source is set to generate about 26 mW of UV power for the MOT. The other one generates up to 50 mW for the 2D-MOT. These power values are far from the maximum achievable. They are the result of a comprise to improve the lifetime of components of the doubling stages (BBO doubling crystals, mirror coatings). While the infrared and visible part of this system prove highly reliable, the 254 nm doubling stages remain the dominant impediment to unattended and daylong continuous operation of our clock. The 2D-MOT increased the cold atom loading rate by factor of 4.5 which gave us leverage to improve clock stability, investigate cold collision shift, operate at a lower trap depth or reduce the vapor pressure in the Hg source region. For instance, we were able to operate a sequence with a cycle time of 482 ms and a duty cycle of 33% giving a short term stability of  $\sim 6.3 \times 10^{-16}$  at 1 s [10] with an ultra-stable laser based on a 10 cm long cavity [11][12]. We have indications that, with we same amount of UV

power, the efficiency of the 2D-MOT could be further increased by optimizing the beam shape. It is reasonable to expect that multiplication by 10 or more of the loading rate would be within reach with such modification and a feasible increase of the power.

These developments and additional improvements to increase the reliability made it possible for our  $^{199}\text{Hg}$  clock to participate to several measurement campaigns in the last years. For instance, the  $^{199}\text{Hg}$  clock was involved in fiber link comparison campaign in May-June 2017 between SYRTE, PTB and NPL. This campaign gave stability measurements between Hg, Sr and  $\text{Yb}^+(\text{E}3)$  that was exploited to search for transient variation of the fine-structure constant and for dark matter [13]. We measured the  $^{199}\text{Hg}/^{87}\text{Sr}$  optical frequency ratio several times during internal and fiber link campaigns in 2017, 2018, 2019, 2020 and 2023, making use of the REFIMEVE fiber network infrastructure [14]. In the last campaign, we could collect about 27 hours of data against the remote Sr clock at PTB. A typical measurement session with optimized parameters reaches a statistical uncertainty of  $2 \times 10^{-17}$  in 2 hours. The successive measurements of the  $^{199}\text{Hg}/^{87}\text{Sr}$  over the years were in good agreement with each others but tend to confirm a discrepancy with the measurement made at RIKEN [2]. A preliminary analysis of the 2023 measurements gives, instead, an agreement with [2]. We are currently trying to confirm these findings and to find the origin of the change. Note that in all these measurements, uncertainties in our Hg clock dominate and our main assumption is that discrepancies and changes come from Hg. The last campaigns shall also provide valuable frequency ratio measurements against one or several  $\text{Yb}^+(\text{E}3)$ ,  $\text{Yb}^+(\text{E}2)$  and Yb clocks, subject to clarifying the Hg/Sr measurements.

The  $^1\text{S}_0$ - $^3\text{P}_0$  clock transition in the fermionic isotope  $^{199}\text{Hg}$  is weakly allowed for electric-dipole transition due to the hyperfine mixing. This same coupling defines the spontaneous emission rate from  $^3\text{P}_0$  to  $^1\text{S}_0$  and the lifetime of the  $^3\text{P}_0$  state. In  $^{199}\text{Hg}$ , the estimated lifetime is rather short ( $\sim 1.5$  s) compared to, for instance, the  $^3\text{P}_0$  lifetime in  $^{87}\text{Sr}$  and  $^{171}\text{Yb}$ . It will be an obstacle to exploit the new generation of ultra-stable lasers like for example the one reported in [15] or [16] or the one that shall result from the work presented section 3. Using bosonic isotopes of Hg provides a means to circumvent this limit. Bosonic isotopes have no nuclear spin and their  $^1\text{S}_0$ - $^3\text{P}_0$  is completely forbidden. The transition can be made weakly allowed by a relatively strong magnetic field as proposed in [17] and experimented in  $^{88}\text{Sr}$  [18][19][20] and  $^{174}\text{Yb}$  [21]. With this quenching method, the strength of the coupling can be adjusted at will and the probing time can be as long as desired to match to the coherence time of the probe laser. We made key developments to use bosonic isotopes of Hg. We developed the means to apply a pulsed and well-controlled quenching magnetic field, using coils of our MOT, an inverting switch and a controlled current source. We have checked that we can apply magnetic field pulse up to 15.5 mT without loosing or perturbing the atomic sample trapped in the lattice. We implemented a widely tunable and flexible probe laser system at 265.6 nm that preserves the low frequency noise properties of our current (flicker noise at  $4 \times 10^{-16}$ ) and future ultra-stable light. Based on an offset phase-locked narrow line fiber laser, this system has the capability to address the  $^1\text{S}_0$ - $^3\text{P}_0$  clock transition of any of the natural isotopes of Hg. We optimized the beam routing and shaping of the 265.6 nm light regenerated by resonant frequency doubling in order to maximize the coupling to atoms held the lattice trap. This optimization and several other tests were made with the help of the  $^{199}\text{Hg}$  fermionic isotope. From the maximum Rabi frequency observed with  $^{199}\text{Hg}$  ( $\sim 2$  kHz) and the other parameters, we infer that we should reach a Rabi frequency of 50 Hz. This is quite small and the search for the transition should be challenging but feasible for the  $^{198}\text{Hg}$  bosonic isotope for which the transition frequency is known with a  $1\sigma$  uncertainty of 10.3 MHz.

Fully exploiting the potential of bosonic isotopes and of new ultra-stable lasers will require to have long probe times, largely longer than the limit imposed by the lattice lifetime observed in our current setup. This is a further motivation for us to reduce the pressure of background gases, which we already mentioned as a limit to our work with  $^{199}\text{Hg}$ . To improve the background

pressure, especially the one of Hg, we developed a home-built cryogenic pump that can be fit to our setup without major modification. The pump consists of two copper plates clamped onto a copper tube through which liquid nitrogen circulates. We estimate that this pump shall have an effective pumping speed at the level of the lattice trap of several  $\text{l.s}^{-1}$  for Hg. We conducted tests that showed a significant positive impact on the vacuum level. We expect that using this device will give us a preliminary means to investigate effects of background gas collisions (frequency shifts and lattice lifetime limitation). And drastic and perennial improvement of vacuum level will then require a major redesign of our setup.

## 2. Non-destructive detection for Sr lattice clocks

Utilizing spin squeezing to overcome the standard quantum limit in order to enhance the clock frequency stability has first been demonstrated in microwave atomic clocks [22]. However, spin squeezing on optical clock transitions is more challenging due to the lack of differential measurement techniques directly accessing the population difference, as well as the lower number of atoms probed in optical clocks, and was accomplished only recently. A first demonstration involved coherently transferring spin-squeezing from a microwave to an optical transition on ytterbium [23]. A very recent work presents a metrological gain of 1.9 dB on a strontium optical lattice clock, relying on the cavity-assisted quantum non-demolition (QND) measurements that works on the near-resonant regime [24].

Here, we propose and realize a different QND measurement scheme in a strontium optical lattice clock, where the clock atoms are trapped and coupled with a far-detuned probe laser in a single spatial cavity mode [25], aiming at integrating the apparatus into the operational clocks. In our scheme, spin-squeezing is produced via cavity-enhanced collective coupling between an ensemble of strontium atoms and a probe laser off-resonant with the  $^1S_0 - ^1P_1$  transition at 461 nm, as depicted in the energy level of Fig. 1. For this, the number of atoms in the electronic ground state  $N_{\downarrow}$  is acquired by a PDH-like heterodyne scheme, in which phase-modulation sidebands are simultaneously injected in two longitudinal modes of the cavity, ensuring both immunity to technical noises (laser frequency noise and mechanical vibrations of the cavity), and homogeneous longitudinal atom-cavity coupling  $g$  [25]. Our latest implementation [26] makes use of two electro-optic phase modulators in order to reach a large atom-light detuning of  $\Delta = \pm 5.5$  GHz, and to decouple the dynamics of the detection scheme from the error signal used to lock the probe beam on the cavity. These two features are critical in order to reach the low photon scattering limit characterizing quantum non-demolition measurements.

Practically, the number of atoms is deduced from a measurement of the frequency shift of the cavity modes, given by  $\delta\omega_c = Ng^2/\Delta$ . For the typical number of probed atoms, this frequency shift is larger than the cavity line-width, making the atomic signal move out of the linear regime (see Fig. 1). To handle this, we feedback the atomic signal to one of the modulation frequencies  $\Omega'$  and record the frequency correction which is equivalent to  $\delta\omega_c$  [27]. With this scheme, we have verified the scaling between  $\delta\omega_c$  and  $N_{\downarrow}$  as measured with an EMCCD camera, and measured the noise limitations in our system, including the quantum projection noises, and the detection noise (electronic noise and photon shot noise).

Besides the detection of the atomic states with QND measurements with a high signal-to-noise ratio, the preservation of the atomic coherence is also mandatory for entering the regime of metrological improvement. For this, the probe power is tuned to ensure a scattered photon rate by one atom as small as  $10^{-2} \gamma/\mu\text{s}$ . However, the atomic coherence still suffers from dephasing with a rate of  $ng^2/\Delta$  ( $n$  is the probe photon number) which comes from the interaction with the probe light. To cancel this effect, we use a photon-echo protocol where a  $\pi$  clock pulse is inserted between two QND measurements with equal detection time to rephase the atomic states which are initially prepared by a  $\pi/2$  clock pulse. By measuring the variation of contrast of Ramsey fringes formed by two time-separated  $\pi/2$  clock pulses due to the non-demolition measurements,

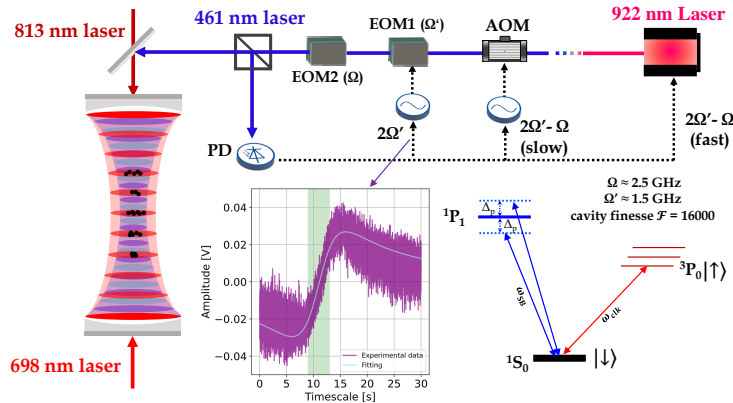


Figure 1: Quantum nondemolition measurements scheme with far-detuning probe laser. Two electro-optic modulators (EOMs) are used to phase-modulate the 461 nm probe laser and flexibly adjust the power of probe sidebands. The modulation frequency frequencies of the two EOMs are  $\Omega = 2.5$  GHz and  $\Omega' = 1.5$  GHz, respectively. An acoustic-optical modulator (AOM) is to match the frequency difference between the cavity resonance and probe laser. Two insets are the atomic signal and the relevant energy levels of strontium.

we observe that the photon-echo method mitigates the decoherence in our apparatus. There is still residual decoherence leading to an additional loss of the contrast by about 1.1 times at our optimal experimental conditions, and which could be further reduced with a more appropriate echo pulse [28].

With an initial preparation of the coherent spin states for around  $2 \times 10^4$  atoms, we conducted two consecutive composited QND measurements to investigate the generation of the spin-squeezing, and the measurement protocol is as presented in Fig 2a. In each measurement, the transition probability which indicates the atomic states is given by  $P^{(i)} = N_{\uparrow}^{(i)} / (N_{\downarrow}^{(i)} + N_{\uparrow}^{(i)})$ , where  $i$  is the measurement order. Because the quantum projection noise which dominates each of the two measurements, is correlated, it can be rejected by a factor of  $1/\chi_{\text{QND}} = (\Delta P_{\text{SQL}} / (\Delta(P_2 - \alpha P_1)))^2$ , where  $\Delta P_{\text{SQL}}$  is the standard deviation of the transition probability in the case of standard quantum limit, and  $\alpha = \text{Cov}(P_1 - P_2) / (\Delta P_1)^2$  represents the conditional correlation coefficient. Generally, a smaller  $\chi_{\text{QND}}$  requires a better signal-to-noise ratio which means stronger probe strength. However, we need to trade off the atomic decoherence. The Wineland parameter  $\xi_w = \chi_{\text{QND}} \cdot C_i / C_f^2$  can be used to represent the metrological improvement, where  $C_i$  ( $C_f$ ) is the Ramsey fringe contrast before (after) the QND measurements. We investigated the  $\xi_w$  at different probe strengths, and the results are shown in Fig. 2b. At a scattered photon number of around 0.2,  $\xi_w < 1$  is obtained, which infers the generation of the spin squeezing. With the further suppression of the atomic decoherence by optimizing the photon-echo protocol, reduction of the additional free-space scattered photons stemming from unwanted coupled sidebands, and enhancement of the signal-to-noise ratio by increasing the coupling efficiency of the probe, it is promising to obtain a considerable metrological improvement based on our scheme for the operational lattice clocks.

### 3. Laser stabilization using spectral hole burning

Given the extraordinary progress in optical lattice clocks, the need of an ultra-stable optical oscillator has become urgent. Whereas the room-temperature high-finesse Fabry-Perot cavity stabilized lasers reach their fundamental thermal noise limited fractional frequency instabilities at the low  $10^{-16}$  around 1 s integration time [30], an improvement by at least one order of magnitude is necessary in order to demonstrate the quantum projection noise limit in optical

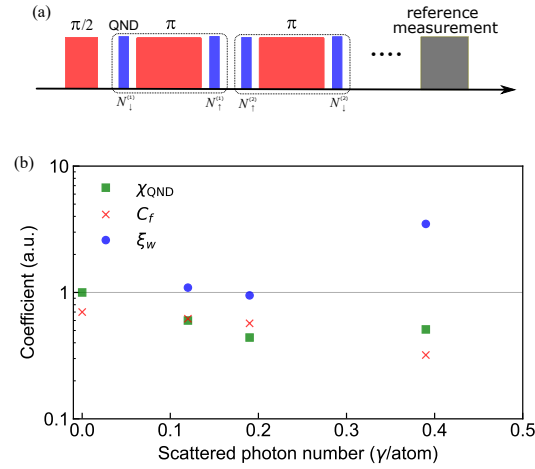


Figure 2: Observation of spin squeezing. (a) measurement protocol for observing the quantum correlations and spin squeezing. The red bar indicates the 698 nm clock laser pulse and the blue bar indicates the 461 nm QND probe pulse. The clock Rabi time is 0.3 ms. (b) at different probe strengths that are calculated from the measured photon scattering rate [29], measurement results for the quantum projection noises reduction coefficient ( $\chi_{\text{QND}}$ , green-square points), the contrast of the Ramsey fringe ( $C_f$ , red-cross points), and the Wineland parameter ( $\xi_w$ , blue-circle points).

lattice clocks with the conventional cyclic operation with dead time in typical situations [31]. Several strategies to lower the thermal noise floor of the Fabry-Perot cavities have been pursued : increasing the size of the optical mode on the mirrors [15], using crystalline material with better thermal mechanical properties for the cavity components [16, 32], going to cryogenic temperatures [33], and a combination of those. However, the outcome is still limited by thermal noise, albeit under new conditions, with the price of added technological complexities, mostly related to cryogenics and vibration management.

It is in this light that we investigate the so-called ‘spectral hole burning’ as an alternative method to derive short-term frequency stabilities. This method is based on the spectroscopy of rare-earth ions doped in a crystalline matrix, by optically pumping and shelving these ions into metastable states to create long-lived spectral structures as frequency references. Since the homogeneous line width is related to the optical coherence time of the excited state, a narrow line laser and an appropriate choice of the dopant and the host, Europium ions doped at 0.1 at% into Yttrium orthosilicate ( $\text{Eu}^{3+}:\text{Y}_2\text{SiO}_5$ , or  $\text{Eu}:\text{YSO}$ ) in our case, allow for the realization of spectral holes with full width at half maxima as low as 3 kHz at about 4 K inside a much broader inhomogeneous profile. The hyperfine splitting of the ground state of the  $\text{Eu}^{3+}$  ions gives rise to a spectral-hole life time on the order of 10 hours near 4 K. The solid-state nature of the crystal ensures a large number of ions participating in spectroscopy, which is favorable for a good signal to noise ratio. Last but not least, the fundamental limits of such a system is unknown, but preliminary estimations, including that of the thermal noise, appear to be low compared to classic Fabry-Perot based systems at room or even cryogenic temperatures.

We use heterodyne interferometry to measure and correct the frequency of a probe laser field with respect to a spectral hole structure [34, 35, 36]. The experimental setup is shown in Fig. 3(a). By the Kramers-Kronig relation, a narrow transmission spectrum of a spectral hole induces a linear dephasing of a nearly resonant laser field, with the zero crossing located at the center frequency of the spectral hole, see Fig. 3(b). We optically beat down the probe signal to the radio frequency (RF) regime, and measure the phase against that collected on a reference

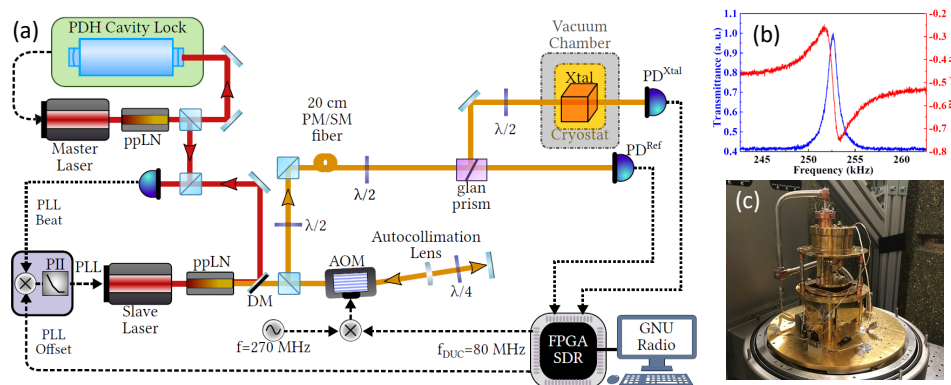


Figure 3: (a) A schematic of the experimental setup of the heterodyne interferometry. Drawing reproduced from [36]. (b) Typical transmittance and dephasing of a narrow spectral hole. (c) The custom fit dilution stage from Pasqal-MyCryoFirm.

path, so as to obtain this dephasing that serves as an error signal for the frequency servo loop. In order to be insensitive to differential noise sources between the two paths, monitor modes can be generated and placed in a broad spectral hole to measure and subtract their contribution from the error signal. Multimode generation also constitutes a means to spread the probing optical power into several narrow spectral holes in order to increase the signal to noise ratio while keeping overburning (continuous optical pumping from the probe laser field) in check.

The technological challenge in multimode generation and detection is overcome by using all digital signal processing, with python-based GNURadio software package coupled with a universal software-defined radio peripheral (USRP), Ettus X310 in our case, that offers phase coherent RF multiple inputs and outputs. Multiple frequency modes in time domain can be generated using inverse fast Fourier transform of the desired spectrum centered on zero frequency. The USRP uses digital up conversion to shift the spectrum to a suitable RF signal to drive an acousto-optic modulator that imprints the multiple frequency modes onto an optical carrier. To detect the phase shift of each modes, the previously mentioned beatnote is measured by suitable photodiodes and sent to the USRP input ports, yielding both the amplitude and the phase information using IQ detection, before being digitally down converted into the base band. A narrow-band polyphase channelizer is used to isolate each frequency component before processing the phase information and generating the error and correction signal. The details of our implementation can be found in [36]. Compared to using only a single probe mode [34], this fully-digital multi-heterodyne approach allows decreasing technical noise sources by orders of magnitudes at 1 s time scale or longer and reaching a detection noise (with optical probing power compatible with hours of continuous operation) of  $2 \times 10^{-16}$  at 1 s, with clear prospects to reach the  $10^{-17}$  range or even lower [36]. Our lowest reported laser frequency instability when locked onto a structure of a narrow spectral hole and a broad one is  $1.7 \times 10^{-15}$  at 1 s so far [35]. We expect further improvements when more narrow spectral holes are used for locking.

With the possibility of tracking the absolute frequency of the spectral holes by measuring the laser frequency, when locked, against the primary frequency standards at the SYRTE laboratory via an optical frequency comb, we have been studying several effects that could potentially impact the short-term stability, namely the sensitivity to a fluctuating DC electric field, mechanical strains (or equivalently accelerations), and the temperature of the crystal.

The measurement of the DC Stark effect is detailed in [37]. Due to the symmetry of the YSO crystal, a spectral hole essentially splits into two with positive and negative frequency shift in the presence of a homogeneous electric field. By analysing both branches for residual

asymmetries, targeting a laser fractional frequency instability at the  $10^{-17}$ , we are able to infer an upper limit for electric field fluctuations to  $2.3 \text{ V.m}^{-1}$  RMS, which is experimentally within reach.

As for the sensitivity to mechanical strains, or equivalently to vibrations, we employed a cryo-compatible 3-axis translation stage in order to place or remove small masses (aluminium plates) on the crystal, while probing the transmission spectrum in the vicinity of a priorly photo-imprinted spectral hole [38, 39]. By characterizing the linear frequency shift, we established the intrinsic acceleration sensitivity to range from  $1.5 \times 10^{-11} (\text{m.s}^{-2})^{-1}$  down to  $1.3 \times 10^{-12} (\text{m.s}^{-2})^{-1}$  (depending on the direction of the strain and the crystal substitution site), giving an upper bound, for a target laser fractional frequency instability of  $10^{-17}$  at 1 s, to the tolerated vibration noise to be below  $10^{-5} \text{ m.s}^{-2}/\sqrt{\text{Hz}}$ , which is manageable even in the presence of a pulse-tube cryocooler that allows for continuous operation without the need of regular replacement of cryogen.

Concerning the impact of the temperature of the crystal  $T$ , based on the two-phonon Raman model, one expects the resonance frequency of rare-earth dopants  $\nu$  to follow a scaling law of  $\nu \propto T^4$  [40]. This is in fact realized only for one of the two substitution sites in Eu:YSO. However, in both cases, the sensitivity to temperature fluctuations near 4 K largely limit the performance achieved in [35]. In the presence of an external isotropic pressure in thermal equilibrium with the crystal, however, the thermal fluctuation induced pressure change would counteract the thermal expansion and contraction of the crystal itself, giving the possibility to cancel to the first order the temperature induced frequency shift of the spectral holes for a well chosen pressure-temperature couple. Similarly to earlier work in [41], we investigated these behaviours at temperatures achievable by our pulsed-tube cryocooler. Whereas we were able to verify the cancellation of the temperature sensitivity in an environment that is coupled to an isotropic pressure [42], the technical challenges in realizing a hermetic gas cell that is robust against temperature cycling is tremendous and requires technical expertise and dedicated effort. Furthermore, this approach is only valid for timescales long-enough where thermal equilibrium is reached. We currently explore an alternative that consists of further decreasing the crystal temperature using a dilution refrigerator, see Fig. 3(c). On one hand, assuming the  $T^4$  scaling, the temperature sensitivity,  $\propto T^3$ , would decrease significantly when the temperature is reduced by an order of magnitude. On the other hand, it is known that the absolute residual temperature fluctuations (in K) at dilution temperatures is lower than that at pulsed-tube temperatures. It is therefore reasonable to expect that the temperature noise induced frequency instability will be well below the target instability of  $10^{-17}$ .

#### 4. Conclusions

We presented developments in three different aspects of optical frequency metrology that have the potential individually, and even more so, when used together, to increase the stability of optical lattice clock beyond the  $1 \times 10^{-17}$  level at 1 s. To this end, one would rely on spectral purity transfer using optical frequency comb to transfer the performance of an ultra-stable laser based on spectral hole burning (discussed in sec. 3) from its specific frequency 517 THz (wavelength of 580 nm) to other relevant frequencies, in our case, the clock transition frequencies of Sr (429 THz) and Hg ( $4 \times 282$  THz) and the frequency of fiber networks (194 THz). It is well-established that such spectral purity transfer can be done at the  $10^{-18}$  level [43]. Such probe lasers used in combination with  $^{87}\text{Sr}$  or a bosonic isotope of Hg (discussed in sec. 1) in a shallow lattice trap shall permit probing time of 1 second, from which one can expect clock instabilities  $\leq 10^{-17} \tau^{-1/2}$ . Further improvement can be expected when making use of non-destructive detection discussed in sec. 2. In [44], we showed theoretically that a simple and practical scheme made of a Rabi interrogation pulse accompanied with 3 non-destructive detection pulses can give significant gain (7.9 dB for  $2 \times 10^4$  detected atoms) when properly

optimized taking into account real imperfections. Another possible use of the non-destructive detection is the so-called atomic phase lock scheme proposed in [45] and tested experimentally with a microwave transition in [46], and with an optical transition in [27]. This scheme makes it possible to extend the probing time beyond the coherence time of the probe laser. With two clocks using the same probe laser (or probe lasers with correlated phase noise via spectral purity transfer), one can also implement a compound clock scheme proposed and tested in [47] where one high-signal-to-noise clock coarsely tracks the phase of the probe laser while the other one makes a high-resolution measurement of the same phase. Like the previous one, the scheme can in principle enable a probing time for the second clock way beyond the coherence time of the laser. These few examples show the potential of the three developments reported here to reach exquisite short term stabilities, when combined together. In turn, instabilities  $\leq 10^{-17}\tau^{-1/2}$  greatly facilitate investigations of systematic shifts below the  $10^{-18}$  level. Alternatively or concurrently, these schemes can be used to reduce some biases, for instance by using them as a means to preserve an excellent stability while reducing the number of atoms and thereby collision shifts. Similarly, some of these schemes could be used to preserve an excellent stability even when using a simplified and less high-performance ultra-stable laser, in the context of technological trade-offs for transportable or industrial clocks. Developments that we described shall permit optical frequency standards and optical frequency ratio measurements with higher accuracy, that will make significant contributions towards fulfilling criteria for the redefinition of the SI second [48], towards uses of optical frequency standards in fundamental physics, and towards emerging applications like chronometric geodesy.

### Acknowledgments

We acknowledge the support from SYRTE's technical services for the development of many electronic, mechanical, vacuum and computer systems involved in the present work. This paper gives a review of work done at SYRTE in the several last years on topics mentioned in the abstract. We acknowledge many essential contributions to the reviewed work from co-authors of articles that we cite in reference for the work carried out at SYRTE.

We acknowledge funding from the Ville de Paris Emergence Program, the Région Ile de France DIM C'nano and SIRTEQ, the LABEX Cluster of Excellence FIRST-TF (ANR-10-LABX-48-01) within the Program "Investissement d'Avenir" operated by the French National Research Agency (ANR), the H2020 QuantERA ERA-NET Cofund QCLOCKS, the European Commission Horizon Europe Framework Programme under the UltraStabLaserViaSHB project under the Marie Skłodowska-Curie grant agreement No GAP-101068547, and from EMPIR under project 17FUN03 USOQS, 15SIB03 OC18 and 20FUN08 NEXTLASERS. EMPIR projects are co-funded by the European Union's Horizon 2020 research and innovation program and the EMPIR participating states. We acknowledge funding from ERC Consolidator Grant AdOC (ERC-2013-CoG-617553).

### References

- [1] Tyumenev R, Favier M, Bilicki S, Bookjans E, Le Targat R, Lodewyck R, Nicolodi D, Le Coq Y, Abgrall M, Guéna J, De Sarlo L and Bize S 2016 *New Journal of Physics* **18** 113002 URL <http://stacks.iop.org/1367-2630/18/i=11/a=113002>
- [2] Yamanaka K, Ohmae N, Ushijima I, Takamoto M and Katori H 2015 *Phys. Rev. Lett.* **114**(23) 230801 URL <https://link.aps.org/doi/10.1103/PhysRevLett.114.230801>
- [3] Recommended values of standard frequencies <https://www.bipm.org/en/publications/mises-en-pratique/standard-frequencies.html>
- [4] Recommendation CCTF PSFS 2 (2021): Updates to the CIPM list of standard frequencies <https://www.bipm.org/en/committees/cc/cctf/22-2-2021>
- [5] Margolis H S, Panfilo G, Petit G, Oates C, Ido T and Bize S 2024 The CIPM list "Recommended values of standard frequencies": 2021 update (*Preprint* 2401.14537) URL <http://arxiv.org/abs/2401.14537>
- [6] Yi L, Mejri S, McFerran J J, Le Coq Y and Bize S 2011 *Phys. Rev. Lett.* **106** 073005

- [7] McGrew W F, Zhang X, Fasano R J, Schäffer S A, Bely K, Nicolodi D, Brown R C, Hinkley N, Milani G, Schioppo M, Yoon T H and Ludlow A D 2018 *Nature* **1** ISSN 1476-4687 URL <https://www.nature.com/articles/s41586-018-0738-2>
- [8] Alves B X R, Foucault Y, Vallet G and Lodewyck J 2019 Background gas collision frequency shift on lattice-trapped strontium atoms *2019 Joint Conference of the IEEE International Frequency Control Symposium and European Frequency and Time Forum (EFTF/IFC)* pp 1–2
- [9] Guo C, Favier M, Galland N, Cambier V, Álvarez-Martínez H, Lours M, De Sarlo L, Andia M, Le Targat R and Bize S 2020 *Review of Scientific Instruments* **91** 033202 ISSN 0034-6748 URL <https://aip.scitation.org/doi/10.1063/1.5140793>
- [10] Guo C, Cambier V, Calvert J, Favier M, Andia M, de Sarlo L and Bize S 2023 *Phys. Rev. A* **107** 033116 URL <https://link.aps.org/doi/10.1103/PhysRevA.107.033116>
- [11] Dawkins S, Chicireanu R, Petersen M, Millo J, Magalhães D, Mandache C, Le Coq Y and Bize S 2010 *Appl. Phys. B: Lasers and Optics* **99**(1) 41 ISSN 0946-2171 URL <http://dx.doi.org/10.1007/s00340-009-3830-3>
- [12] Millo J, Magalhaes D V, Mandache C, Coq Y L, English E M L, Westergaard P G, Lodewyck J, Bize S, Lemonde P and Santarelli G 2009 *Phys. Rev. A* **79** 053829 URL <http://link.aps.org/abstract/PRA/v79/e053829>
- [13] Roberts B M, Delva P, Al-Masoudi A, Amy-Klein A, Bærentsen C, Baynham C F A, Benkler E, Bilicki S, Bize S, Bowden W, Calvert J, Cambier V, Cantin E, Curtis E A, Dörscher S, Favier M, Frank F, Gill P, Godun R M, Grosche G, Guo C, Hees A, Hill I R, Hobson R, Huntemann N, Kronjäger J, Koke S, Kuhl A, Lange R, Legero T, Lipphardt B, Lisdat C, Lodewyck J, Lopez O, Margolis H S, Álvarez-Martínez H, Meynadier F, Ozimek F, Peik E, Pottie P E, Quintin N, Sanner C, Sarlo L D, Schioppo M, Schwarz R, Silva A, Sterr U, Tamm C, Targat R L, Tuckey P, Vallet G, Waterholter T, Xu D and Wolf P 2020 *New J. Phys.* **22** 093010 ISSN 1367-2630 URL <https://doi.org/10.1088/1367-2630/abaace>
- [14] See the invited presentation of A. Amy-Klein et al., *REFIMEVE frequency and time network and applications* at the 2023 Symposium on Frequency Standards and Metrology and: URL <https://www.refimeve.fr/index.php/en/>
- [15] Häfner S, Falke S, Grebing C, Vogt S, Legero T, Merimaa M, Lisdat C and Sterr U 2015 *Opt. Lett.* **40** 2112–2115 URL <http://ol.osa.org/abstract.cfm?URI=ol-40-9-2112>
- [16] Matei D G, Legero T, Häfner S, Grebing C, Weyrich R, Zhang W, Sonderhouse L, Robinson J M, Ye J, Riehle F and Sterr U 2017 *Phys. Rev. Lett.* **118** 263202 URL <https://link.aps.org/doi/10.1103/PhysRevLett.118.263202>
- [17] Taichenachev A V, Yudin V I, Oates C W, Hoyt C W, Barber Z W and Hollberg L 2006 *Phys. Rev. Lett.* **96** 083001 (pages 4) URL <http://link.aps.org/abstract/PRL/v96/e083001>
- [18] Baillard X, Fouché M, Targat R L, Westergaard P G, Lecallier A, Coq Y L, Rovera G D, Bize S and Lemonde P 2007 *Opt. Lett.* **32** 1812 URL <https://doi.org/10.1364/OL.32.001812>
- [19] Origlia S, Pramod M S, Schiller S, Singh Y, Bongs K, Schwarz R, Al-Masoudi A, Dörscher S, Herbers S, Häfner S, Sterr U and Lisdat C 2018 *Phys. Rev. A* **98** 053443
- [20] Takano T, Mizushima R and Katori H 2017 *Appl. Phys. Express* **10** 072801 ISSN 1882-0778
- [21] Barber Z W, Hoyt C W, Oates C W, Hollberg L, Taichenachev A V and Yudin V I 2006 *Phys. Rev. Lett.* **96**(8) 083002 URL <http://link.aps.org/doi/10.1103/PhysRevLett.96.083002>
- [22] Hosten O, Engelsen N J, Krishnakumar R and Kasevich M A 2016 *Nature* **529** 505–508
- [23] Pedrozo-Peñafiel E, Colombo S, Shu C, Adiyatullin A F, Li Z, Mendez E, Braverman B, Kawasaki A, Akamatsu D, Xiao Y et al. 2020 *Nature* **588** 414–418
- [24] Robinson J M, Miklos M, Tso Y M, Kennedy C J, Bothwell T, Kedar D, Thompson J K and Ye J 2024 *Nature Physics* **20** 208–213
- [25] Vallet G, Bookjans E, Eismann U, Bilicki S, Le Targat R and Lodewyck J 2017 *New Journal of Physics* **19** 083002
- [26] Shang H, Marin M A C, Foucault Y, Le Targat R and Lodewyck J 2022 Quantum nondemolition detection for strontium optical lattice clock *2022 Joint Conference of the European Frequency and Time Forum and IEEE International Frequency Control Symposium (EFTF/IFCS)* (IEEE) pp 1–3
- [27] Bowden W, Vianello A, Hill I R, Schioppo M and Hobson R 2020 *Physical Review X* **10** 041052
- [28] Huang M Z, de la Paz J A, Mazzoni T, Ott K, Rosenbusch P, Sinatra A, Garrido Alzar C L and Reichel J 2023 *PRX Quantum* **4** 020322 ISSN 2691-3399
- [29] Lodewyck J, Westergaard P G and Lemonde P 2009 *Physical Review A* **79** 061401
- [30] Numata K, Kemery A and Camp J 2004 *Physical Review Letters* **93** 250602
- [31] Nicholson T L, Martin M J, Williams J R, Bloom B J, Bishof M, Swallows M D, Campbell S L and Ye J 2012 *Physical Review Letters* **109** 230801
- [32] Cole G D, Zhang W, Martin M J, Ye J and Aspelmeyer M 2013 *Nature Photonics* **7** 644–650 ISSN 1749-4893

- [33] Robinson J M, Oelker E, Milner W R, Zhang W, Legero T, Matei D G, Riehle F, Sterr U and Ye J 2019 *Optica* **6** 240–243
- [34] Gobron O, Jung K, Galland N, Predehl K, Le Targat R, Ferrier A, Goldner P, Seidelin S and Le Coq Y 2017 *Optics Express* **25** 15539–15548
- [35] Galland N, Lučić N, Zhang S, Alvarez-Martinez H, Le Targat R, Ferrier A, Goldner P, Fang B, Seidelin S and Le Coq Y 2020 *Optics letters* **45** 1930–1933
- [36] Lin X, Hartman M T, Zhang S, Seidelin S, Fang B and Le Coq Y 2023 *Opt. Expr.* **31** 38475
- [37] Zhang S, Lučić N, Galland N, Le Targat R, Goldner P, Fang B, Seidelin S and Le Coq Y 2020 *Applied Physics Letters* **117** 221102
- [38] Galland N, Lučić N, Fang B, Zhang S, Le Targat R, Ferrier A, Goldner P, Seidelin S and Le Coq Y 2020 *Phys. Rev. Applied* **13** 044022
- [39] Zhang S, Galland N, Lučić N, Le Targat R, Ferrier A, Goldner P, Fang B, Le Coq Y and Seidelin S 2020 *Physical Review Research* **2** 013306
- [40] Könz F, Sun Y, Thiel C W, Cone R L, Equall R W, Hutcheson R L and Macfarlane R M 2003 *Phys. Rev. B* **68** 085109
- [41] Thorpe M J, Rippe L, Fortier T M, Kirchner M S and Rosenband T 2011 *Nature Photonics* **5** 688–693
- [42] Zhang S, Seidelin S, Le Targat R, Goldner P, Fang B and Le Coq Y 2023 *Phys. Rev. A* **107**(1) 013518
- [43] Nicolodi D, Argence B, Zhang W, Le Targat R, Santarelli G and Le Coq Y 2014 *Nat Photon* **8** 219 ISSN 1749-4893 URL <http://dx.doi.org/10.1038/nphoton.2013.361>
- [44] Orenes D B, Sewell R J, Lodewyck J and Mitchell M W 2022 *Phys. Rev. Lett.* **128** 153201 URL <https://link.aps.org/doi/10.1103/PhysRevLett.128.153201>
- [45] Shiga N, Mizuno M, Kido K, Phoonthong P and Okada K 2014 *New Journal of Physics* **16** 073029 URL <http://stacks.iop.org/1367-2630/16/i=7/a=073029>
- [46] Kohlhaas R, Bertoldi A, Cantin E, Aspect A, Landragin A and Bouyer P 2015 *Phys. Rev. X* **5**(2) 021011 URL <http://link.aps.org/doi/10.1103/PhysRevX.5.021011>
- [47] Dörscher S, Al-Masoudi A, Bober M, Schwarz R, Hobson R, Sterr U and Lisdat C 2020 *Communications Physics* **3** 1–9 ISSN 2399-3650 URL <http://www.nature.com/articles/s42005-020-00452-9>
- [48] Dimarcq N, Gertszov M, Mileti G, Bize S, Oates C W, Peik E, Calonico D, Ido T, Tavella P, Meynadier F, Petit G, Panfilo G, Bartholomew J, Defraigne P, Donley E A, Hedekvist P O, Sesia I, Wouters M, Dubé P, Fang F, Levi F, Lodewyck J, Margolis H S, Newell D, Slyusarev S, Weyers S, Uzan J P, Yasuda M, Yu D H, Rieck C, Schnatz H, Hanado Y, Fujieda M, Pottie P E, Hanssen J, Malimon A and Ashby N 2024 *Metrologia* **61** 012001 ISSN 0026-1394 URL <https://dx.doi.org/10.1088/1681-7575/ad17d2>